

# JCTC

## Journal of Chemical Theory and Computation

### Conceptual Density-Functional Theory for General Chemical Reactions, Including Those That Are Neither Charge- nor Frontier-Orbital-Controlled. 2. Application to Molecules Where Frontier Molecular Orbital Theory Fails

James S. M. Anderson,<sup>†</sup> Junia Melin,<sup>‡</sup> and Paul W. Ayers<sup>\*,†</sup>

*Department of Chemistry, McMaster University, Hamilton, Ontario, Canada L8S 4M1,  
and Department of Chemistry, Kansas State University,  
Manhattan, Kansas 66506-3701*

Received May 10, 2006

**Abstract:** This paper examines cases where frontier molecular orbital theory is known to fail, specifically electrophilic aromatic substitution reactions on isoquinoline and borazarophenanthrenes. While we are able to explain the experimental regioselectivity preferences for isoquinoline without too much difficulty, describing the regioselectivity of the borazarophenanthrenes is much more challenging. This is attributed to the fact that these molecules lie between the electrostatic (or charge) control and electron-transfer (or frontier-orbital) control paradigms. These molecules can, however, be described using the general-purpose reactivity indicator introduced in the first paper of this series. The variation of the general-purpose reactivity indicator with respect to the parameters is readily summed up using what we term “reactivity transition tables”, which provide a compact summary of which products form under different reaction conditions. For the otherwise problematic molecules considered here, the new reactivity indicator performs better than either the Fukui function or the electrostatic potential alone.

#### I. Introduction

In the first paper in this series,<sup>1</sup> the authors derived a general-purpose reactivity indicator that is capable of describing not only electrostatically (or charge) controlled reactions and electron-transfer- (or frontier-orbital-) controlled reactions<sup>2</sup> but also reactions that lie between these two extremes. This paper will apply this reactivity indicator to a particularly challenging set of molecules, where ordinary reactivity predictors have been observed to fail.

Before applying the reactivity indicator, we briefly summarize the results from the first paper in this series. The goal of the first paper was to derive a reactivity indicator that could truly be called a “general-purpose” reactivity indicator. That is, we sought a reactivity indicator that

describes the full spectrum of chemical reactivity, from strong electrostatic control (minimum Fukui function is good), to joint electrostatic and electron-transfer control (maximum Fukui function is good), to strong electron-transfer control [maximum Fukui function is good, but maximum (for nucleophiles) or minimum (for electrophiles) electrostatic potential is also good]. To achieve this goal, we used a perturbative expansion about the separated reagent limit to derive an expression for the interaction energy between an electrophile and a nucleophile (see eq 21 in part 1).

To derive a reactivity indicator, we introduced a single reactive-site interaction model for electrophiles and nucleophiles. In this model, the reactive site of the attacking electrophile/nucleophile is modeled with a point charge and a condensed Fukui function. Inserting this model in the expression for the interaction energy and performing a careful error analysis led to the desired indicators. One of our indicators is appropriate for predicting where an electrophile will attack a nucleophile

\* Corresponding author fax: (905) 522-2509; e-mail: ayers@mcmaster.ca.

<sup>†</sup> McMaster University.

<sup>‡</sup> Kansas State University.

$$\Xi_{\Delta N \leq 0}^{\kappa}(r) \equiv (\kappa + 1) \Phi_{\text{nucleophile}}(r) - \Delta N(\kappa - 1) v_{\text{nucleophile}}^{f-}(r) \quad (1)$$

The other indicator is appropriate for predicting where a nucleophile will attack an electrophile

$$\Xi_{\Delta N \geq 0}^{\kappa}(r) \equiv -(\kappa + 1) \Phi_{\text{electrophile}}(r) + \Delta N(\kappa - 1) v_{\text{electrophile}}^{f+}(r) \quad (2)$$

Because these indicators model the interaction energy of the molecule, the molecule is most reactive in the places where  $\Xi_{\Delta N}^{\kappa}(r)$  is the most negative.

By simply varying the value of  $\kappa$ , the entire spectrum of chemical reactivity can be described, ranging from strong electrostatic control ( $\kappa > 1$ ), to pure electrostatic control ( $\kappa = 1$ ), to joint control by electrostatics and electron-transfer effects ( $-1 < \kappa < 1$ ), to pure electron-transfer control ( $\kappa = -1$ ), to strong electron-transfer control ( $\kappa < -1$ ). The value of  $\kappa$  that is appropriate for a particular reaction can be estimated using the approximate proportionalities:

$$\begin{aligned} \kappa &\approx q_{\text{electrophile}}^{(0)} + \Delta N f_{\text{electrophile}}^{(+)} && \text{for nucleophiles} \\ \kappa &\approx -q_{\text{nucleophile}}^{(0)} - \Delta N f_{\text{nucleophile}}^{(-)} && \text{for electrophiles} \end{aligned} \quad (3)$$

The constant of proportionality is positive and, on the basis of our experience, has order of magnitude 1.

The reactivity indicators in eqs 1 and 2 also depend on the extent of electron transfer. The amount of electron transfer could be computed by minimizing the expression for the interaction energy directly, but the simple formula proposed by Parr and Pearson should be adequate for qualitative purposes<sup>3</sup>

$$\begin{aligned} \Delta N_{\text{electrophile}} &\approx \frac{\mu_{\text{nucleophile}} - \mu_{\text{electrophile}}}{\eta_{\text{nucleophile}} + \eta_{\text{electrophile}}} \\ &\approx \frac{(I_{\text{nucleophile}} - I_{\text{electrophile}}) + (A_{\text{nucleophile}} - A_{\text{electrophile}})}{2(I_{\text{nucleophile}} + I_{\text{electrophile}} - A_{\text{nucleophile}} - A_{\text{electrophile}})} \end{aligned} \quad (4)$$

In this equation,  $\mu$  denotes the electronic chemical potential<sup>4</sup> and  $\eta$  denotes the chemical hardness.<sup>3</sup> The second line of this equation approximates the chemical potential and chemical hardness using the vertical ionization potential ( $I$ ) and vertical electron affinity ( $A$ ) of the reagents. Because nucleophiles transfer electrons to electrophiles, we have chosen a sign convention where  $\Delta N \leq 0$  for nucleophiles and  $\Delta N \geq 0$  for electrophiles. The molecules we are studying in this paper are nucleophiles, so it is the  $\Delta N \leq 0$  case that is of greatest interest here.

The general-purpose reactivity indicators are seen to have a dependence on the Fukui potential,  $v^{\pm}(r)$ , and the molecular electrostatic potential,  $\Phi(r)$ . The electrostatic potential is essential for describing reactions that are electrostatically controlled ( $\kappa = 1$ ); the Fukui potential is essential for describing reactions that are electron-transfer-controlled ( $\kappa = -1$ ). In all other cases, both the electrostatic potential and the Fukui potential play a role in determining a molecule's regioselectivity preferences.

It is useful to approximate the electrostatic potential and the Fukui functions using atomic charges<sup>5,6</sup>

$$\Phi^{(0)}(r) \sim \sum_{\alpha} \frac{q_{\alpha}^{(0)}}{|r - R_{\alpha}|} \quad (5)$$

$$\begin{aligned} v^{f-}(r) &\sim \sum_{\alpha} \frac{f_{\alpha}^{-}}{|r - R_{\alpha}|} \\ v^{f+}(r) &\sim \sum_{\alpha} \frac{f_{\alpha}^{+}}{|r - R_{\alpha}|} \end{aligned} \quad (6)$$

where  $q_{\alpha}^{(0)}$  denotes the atomic charges on the reagent.  $f_{\alpha}^{+}$  and  $f_{\alpha}^{-}$  are the condensed Fukui functions. Using these results, one can derive a condensed version of the indicators in eqs 1 and 2

$$\begin{aligned} \Xi_{\Delta N \leq 0}^{\kappa}(r_p) &\sim \sum_{\alpha \in \text{nucleophile}} \frac{\Xi_{\Delta N \leq 0, \alpha}^{\kappa}}{|r - R_{\alpha}|} \\ \Xi_{\Delta N \leq 0, \alpha}^{\kappa} &= (\kappa + 1) q_{\text{nucleophile}, \alpha}^{(0)} - \Delta N(\kappa - 1) f_{\text{nucleophile}, \alpha}^{-} \end{aligned} \quad (7)$$

$$\begin{aligned} \Xi_{\Delta N \geq 0}^{\kappa}(r_p) &\sim \sum_{\alpha \in \text{electrophile}} \frac{\Xi_{\Delta N \geq 0, \alpha}^{\kappa}}{|r - R_{\alpha}|} \\ \Xi_{\Delta N \geq 0, \alpha}^{\kappa} &= -(\kappa + 1) q_{\text{electrophile}, \alpha}^{(0)} + \Delta N(\kappa - 1) f_{\text{electrophile}, \alpha}^{+} \end{aligned} \quad (8)$$

For special cases, this reactivity indicator recovers the reactivity patterns that would be predicted on the basis of the Fukui function ( $\kappa = -1$ ) or the electrostatic potential ( $\kappa = 1$ ) alone. The new indicator has no value, then, unless it supersedes the description of chemical reactivity that is possible using these reactivity indicators in isolation. This suggests that the new indicator might be useful for studying molecules where frontier molecular orbital theory (FMO) would be expected to work but has been observed to fail. The regioselectivity of electrophilic aromatic substitution reactions is usually well-described using both FMO and density functional theory analogues to frontier molecular orbital theory like the Fukui function.<sup>7-9</sup> This is not always true, however: Dewar showed that FMO fails to describe electrophilic aromatic substitution in isoquinoline, 10-hydroxy-10,9-borazarophenanthrene, and 10-methyl-10,9-borazarophenanthrene. The question arises: does the Fukui function,<sup>10-12</sup> which extends the frontier molecular orbital theory but is nonetheless motivated by FMO ideas, fail in the same way? In section III, it is observed that, while the Fukui function does seem to work better than FMO for these molecules, it still fails to adequately describe their reactivity. (That is, the Fukui function fails "in the same way" as FMO, but not as badly.)

The Fukui function is intimately linked to the idea of electron transfer, so it is an appropriate indicator for "electron-transfer-controlled" (also called frontier-orbital-

controlled and Fukui-function-controlled) reactions. When hard reagents interact, electron transfer is either limited or occurs late in the chemical reaction profile; such reactions are usually called “electrostatically controlled” or “charge-controlled”.<sup>2</sup> The electrostatic potential is a more appropriate indicator than the Fukui function in these cases.<sup>13</sup> Because the Fukui function fails to adequately describe the reactivity of these molecules, perhaps the electrostatic potential will suffice. The results in section III show that the electrostatic potential does not describe the reactivity of these molecules either.

These results suggest that the electrophilic substitution on borazarophenanthrenes represents a difficult, but otherwise suitable, test for the general-purpose reactivity indicator,  $\Xi_{\Delta N \leq 0, \alpha}^K$ , that we derived and discussed in the first paper of this series. Indeed, the theoretical developments in the first paper were motivated by our inability to describe these molecules using ordinary reactivity indicators. Section III contains the main results; we observe that  $\Xi_{\Delta N \leq 0, \alpha}^K$  does an excellent job of describing a variety of electrophilic aromatic substitution reactions on borazarophenanthrenes. Before presenting our results, however, we need to state our computational methods.

## II. Computational Methods

To demonstrate the power of these indicators, we decided to analyze molecules where Dewar found contradictions to frontier molecular orbital effects.<sup>14</sup> In what follows, all calculations were conducted using Gaussian 03<sup>15</sup> and the B3LYP<sup>16–18</sup> functional with the 6-31++G\* basis set.<sup>19</sup> Figures were generated using GaussView 3.0. The atomic charges used to compute condensed reactivity indicators were obtained from four different methods: the Mulliken population analysis<sup>20–23</sup> and natural population analysis (NPA)<sup>24–26</sup> approaches to partitioning the density matrix and the Merz–Singh–Kollman<sup>27,28</sup> (MSK) and CHelpG<sup>29</sup> (CHG) methods for fitting the electrostatic potential.

## III. Results and Discussion

**A. Overview.** We will explore three of the molecules (isoquinoline, 10-hydroxy-10,9-borazarophenanthrene, and 10-methyl-10,9-borazarophenanthrene) Dewar gave as examples where FMO fails to adequately describe regioselectivity.<sup>14</sup> (Dewar gave a fourth example, nitrobenzene. This molecule has been extensively studied using reactivity indicators associated with conceptual DFT and will not be revisited here. More information on nitrobenzene can be found, for example, in the paper of Langenaeker et al.<sup>7</sup>)

For each molecule, we will first present the experimentally observed reactivity preferences. Then, we will present the reactivity preferences predicted by FMO (which predicts that electrophilic attack occurs where the magnitude of the highest occupied molecular orbital is largest), electrostatic considerations (which predicts that electrophilic attack occurs where the electrostatic potential is most negative), and the Fukui function (which predicts that electrophilic attack occurs where  $f^-(r)$  is the largest). When no single method can predict the observed reactivity, we will examine the more general

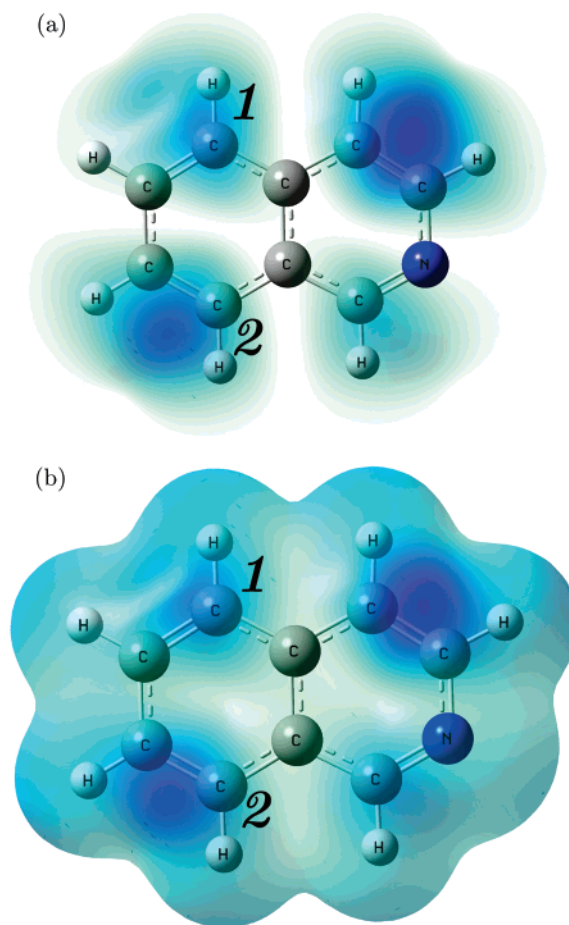
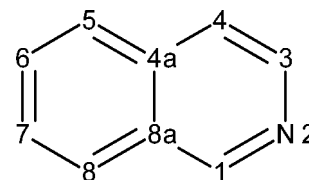


**Figure 1.** (a) Square magnitude of the HOMO orbital,  $|\phi_{\text{HOMO}}(r)|^2$ , (b) the Fukui function from below,  $f^-(r)$ , is plotted on the 0.0004 isodensity surface of the isoquinoline molecule. The molecule should be most reactive where these functions are the largest. The numbers denote the experimentally observed reactivity preferences.<sup>30</sup>

index,  $\Xi_{\Delta N \leq 0, \alpha}^K$ , which combines information from the electrostatic potential and the Fukui function.

**B. Isoquinoline.** Experimental studies on isoquinoline<sup>30</sup>



have shown that the most reactive site of this molecule is carbon 5, with secondary reactivity at carbon 8. Products from electrophilic substitution on carbon 4 were not found, so this site is believed to be unreactive. Figure 1a reports the value of the highest occupied molecular orbital density,  $|\phi_{\text{HOMO}}(r)|^2$ , on the van der Waals surface of the molecule. We model the van der Waals surface with the  $\rho(r) = 0.0004$  isodensity surface; this models the reactive surface of the molecule and is an appropriate indicator of site selectivity.<sup>31–33</sup> In accord with Dewar’s FMO analysis, an electrophilic attack is predicted to occur on the double bonds between carbons 3 and 4, then carbons 7 and 8, and finally carbons 5 and 6. This reactivity order is reversed relative the experimental

products: carbon 5 is the primary reaction site; carbon 8 is the secondary reaction site, and carbon 4 is unreactive.

Sometimes, orbital relaxation effects are important for describing chemical reactivity, and so the Fukui function (which includes orbital relaxation effects)<sup>11</sup> sometimes performs better than  $|\phi_{\text{HOMO}}(r)|^2$  for predicting sites of electrophilic attack. Orbital relaxation effects have been shown to be important in electrophilic aromatic substitution<sup>7</sup> and electrophilic attack on double bonds (in organic molecules)<sup>31</sup> and multiple bonds (in inorganic complexes with metal–metal bonds).<sup>32</sup> It seems plausible, then, that the Fukui function will locate the appropriate sites for electrophilic attack on isoquinoline. To investigate this possibility, we plotted the value of the Fukui function on the molecular van der Waals surface (see Figure 1b). While the Fukui function and  $|\phi_{\text{HOMO}}(r)|^2$  are quantitatively different, they are qualitatively similar: the Fukui function at carbon 4 is slightly larger than that at carbon 8, which is significantly larger than the Fukui function at the dominant reaction site (carbon 5). It is interesting that this trend is altered somewhat if condensed Fukui functions are used. With condensed Fukui functions and ChelpG charges, we have  $f_{\text{C5}} = 0.229$ ,  $f_{\text{C4}} = 0.193$ , and  $f_{\text{C8}} = 0.165$ . While carbon 4 is still predicted to be reactive, at least the first-choice reaction site is now identified correctly. To the best of our knowledge, this is the first molecule where condensed Fukui functions perform decisively better than Fukui functions plotted on a reactive surface. In this case, the Fukui function on carbon 5 is concentrated near the nucleus, and thus, while the Fukui potential (which depends on the total size of the Fukui function in the vicinity of the atom) will be large in the region of carbon 5, the amplitude of the Fukui function [which decays exponentially, rather than as  $(1/r)$ ] has decreased almost to zero on the reactive surface. Thus chastened, we will henceforth focus on condensed reactivity indicators.

For reactions between hard molecules, the appropriate indicator of site selectivity is the electrostatic potential. This is clear already from the works of Klopman and Berkowitz<sup>2,34</sup> but is also a topic of recent emphasis in the conceptual DFT literature.<sup>13,35,36</sup> It follows very clearly from our analysis also, because the extent of electron transfer

$$\Delta N_{\text{nucleophile}} \approx \frac{\mu_{\text{electrophile}} - \mu_{\text{nucleophile}}}{\eta_{\text{electrophile}} + \eta_{\text{nucleophile}}} \quad (9)$$

will be small when the hardness of the reagents is large. When  $|\Delta N|$  is small, the dominant contribution to both  $\Xi_{\Delta N \leq 0}^{\kappa}(r_p)$  and  $\Xi_{\Delta N \geq 0}^{\kappa}(r_p)$  is from the molecular electrostatic potential. While isoquinoline is not especially hard, insofar as the Fukui function has failed to successfully describe its reactivity, it seems desirable to explore the electrostatic potential. This is done by computing the atomic charges, which represent the “condensed” electrostatic potential (cf. eq 5).<sup>37</sup> The charges from several different population analysis schemes are plotted in Figure 2a. The Mulliken charges are manifestly unreliable, as is to be expected for a basis set including diffuse functions. Henceforth, we will not report the results from the Mulliken population analysis. The other charge schemes reported in Figure 2a are more

reasonable, with the two methods of electrostatic potential fitting (MSK and CHG) giving similar results. The NPA scheme is less similar, which may also be due to this method’s stronger dependence on the basis set or due to the fact that NPA, unlike MSK and CHG, is based on a population analysis of the density matrix, and not on fitting the electrostatic potential.

Recall that the reactive site of strong electrophiles is usually positively charged. Electrophilic attack thus tends to occur at the most negatively charged sites of the nucleophile. Looking at Figure 2a, it is clear that the most negative sites in the molecule are the nitrogen atom and carbon 4. Carbon 4, however, is unreactive. The charges on carbon 5 (the most reactive position) and carbon 8 (the second most reactive position) are not especially small.

Sometimes, one argues that one should add the charges of hydrogen atoms into the charges of the atoms they are bonded to. This seems especially useful in electrostatic fitting procedures: because the carbon–hydrogen bond is short, it can be difficult to determine how to partition a reactive carbon’s charge between the carbon atom and the adjacent hydrogen. More generally, the regioselectivity of a molecule is usually determined by interactions that occur when the molecular substrate and the attacking reagent are in van der Waals contact. Because the separation between the molecules is much larger than the length of a carbon–hydrogen bond, from the perspective of the attacking reagent,  $-\text{CH}_n$  groups appear as a single point charge. On the basis of this reasoning, it is preferable to consider “functional group” charges that are computed by adding the charges of hydrogen atoms to the charges of the adjacent “heavy” atom. These data are reported in Figure 2b. Unfortunately, this does not alter the fact that carbon 4 is predicted to be reactive, while the molecular sites that actually are reactive are predicted to be relatively unreactive.

Further thought about the chemistry of isoquinoline rectifies these unsuccessful predictions. Isoquinoline is relatively basic,  $\text{p}K_{\text{b}} = 8.6$ . (Unsurprisingly, this is similar to the  $\text{p}K_{\text{b}}$  of pyridine, which is 8.7.) Experimentally, it is difficult to perform an electrophilic substitution reaction on pyridine: electrophiles are Lewis acids, and so the solutions used for electrophilic aromatic substitutions are also acidic.<sup>38</sup> The experimental studies of Dewar were carried out in a mixture of nitric and sulfuric acids!<sup>30</sup> Even when less extreme conditions are used, the pH of those solutions is almost always less than 5.3, and in that environment, pyridine is protonated. Clearly, performing an electrophilic attack on a protonated molecule will be difficult! Isoquinoline, which is marginally less basic than pyridine, is also expected to be in its protonated state when it undergoes electrophilic aromatic substitution. On the basis of this logic, we performed calculations on protonated isoquinoline.<sup>39</sup> The atomic charges are reported in Figure 3a (raw charges) and 3b (summed with adjacent hydrogens). The condensed Fukui functions are reported in Figure 4a (computed from atomic charges) and 4b (computed from atomic charges summed with adjacent hydrogens). On the basis of the charges, we would predict that the reaction occurs at carbon 5, with carbon 8 and carbon 4 having similar reactivity. On the basis



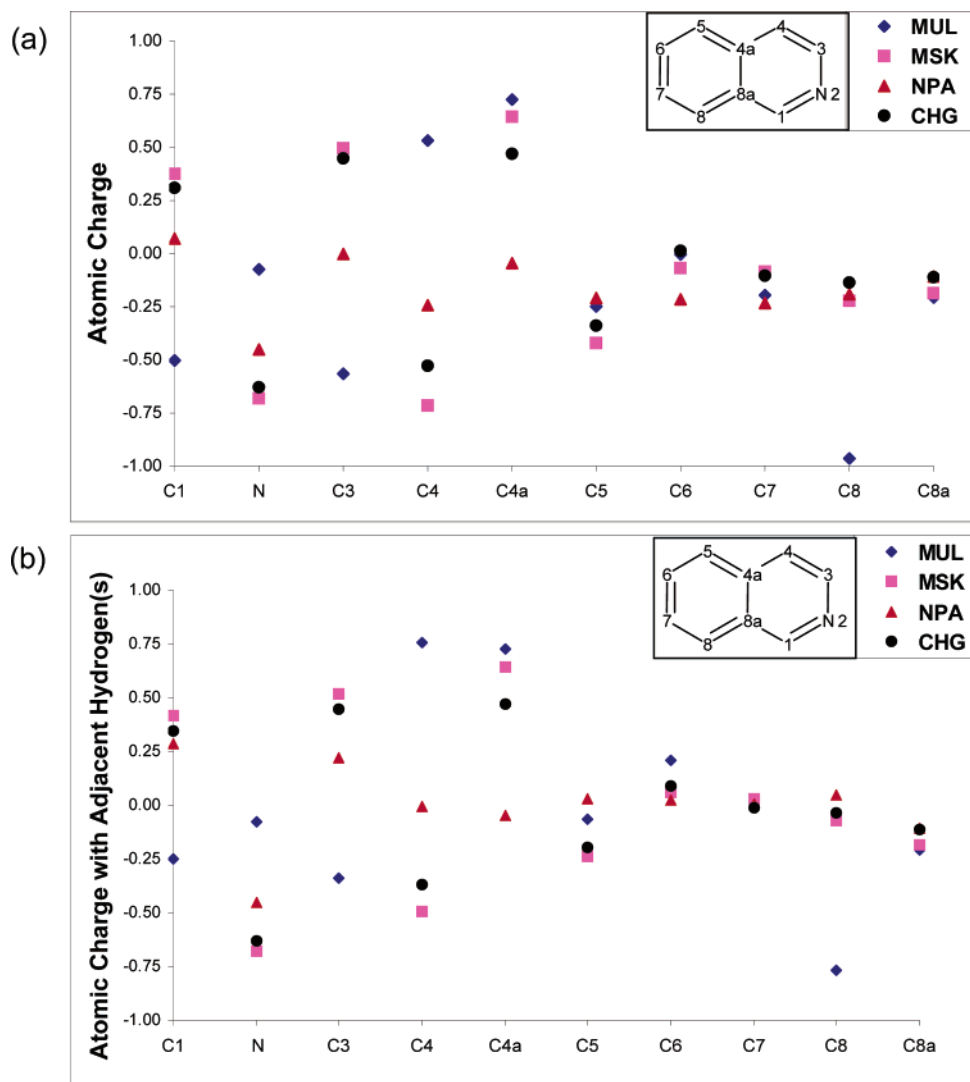


**Figure 2.** Atomic charges (condensed electrostatic potential) of isoquinoline. (a) The atomic charges on the indicated atoms. (b) The atomic charges on the indicated atoms plus the charges of hydrogen atoms bonded to those atoms. The atomic numbering scheme is included as an inset. Experimentally, C5 is the most reactive, followed by C8. C4 is unreactive.

of the Fukui function, we would predict that carbon 5 and carbon 8 are both highly reactive (carbon 5 perhaps slightly more so) and that carbon 4 is not very reactive. This agrees with the experiment: the substantial negative charge on carbon 5, coupled with its significant Fukui function, makes this site highly susceptible to electrophilic attack. Carbon 8 is also favorable electrostatically and on the basis of its Fukui function, but its less negative charge is associated with slightly diminished reactivity. Carbon 4 is not significantly reactive compared to carbon 5 or carbon 8.

Perhaps protonating isoquinoline is too strong an assumption. One could, after all, carry out an electrophilic substitution in an aprotic solvent. To explore this possibility, we considered the complex of pyridine with the sodium cation, which is an extremely weak Lewis acid (see Figure 5). In this case, carbon 4 remains the most negatively charged reactive site. However, the Fukui function is highly concentrated on carbon 5 and, to a lesser extent, carbon 8. Because isoquinoline is not especially hard, it seems reasonable to infer that, under any reasonable set of experimental conditions, the “ion-paired isoquinoline” that is subject to chemical

reaction will react first at carbon 5, with a secondary product associated with reaction at carbon 8.

We could apply our general-purpose reactivity indicator to isoquinoline, but the picture that emerges is quite boring because the electrostatically favored and electron-transfer-favored sites on protonated isoquinoline are the same. Instead, we will apply our reactivity indicator to a much more challenging problem: electrophilic aromatic substitution on 10,9-borazarophenanthrenes.

**C. 10-R-10,9-Borazarophenanthrene. 1. Summary of Experimental Observations.** In addition to isoquinoline, Dewar also pointed out two, more challenging, molecules where experimental results were not in accord with frontier molecular orbital theory. Experimental studies of 10-R-10,9-borazarophenanthrene ( $R = \text{OH}$  or  $\text{CH}_3$ ) indicate that carbon 8 and carbon 6 are both susceptible to electrophilic attack.<sup>40–42</sup> Chlorination of 10-methyl-10,9-borazarophenanthrene favors carbon 8 over carbon 6,<sup>42</sup> while chlorination of 10-hydroxy-10,9-borazarophenanthrene gives the disubstituted product corresponding to reaction at both carbon 6 and carbon 8.<sup>41</sup> Nitration produces a mixture of the products associated with

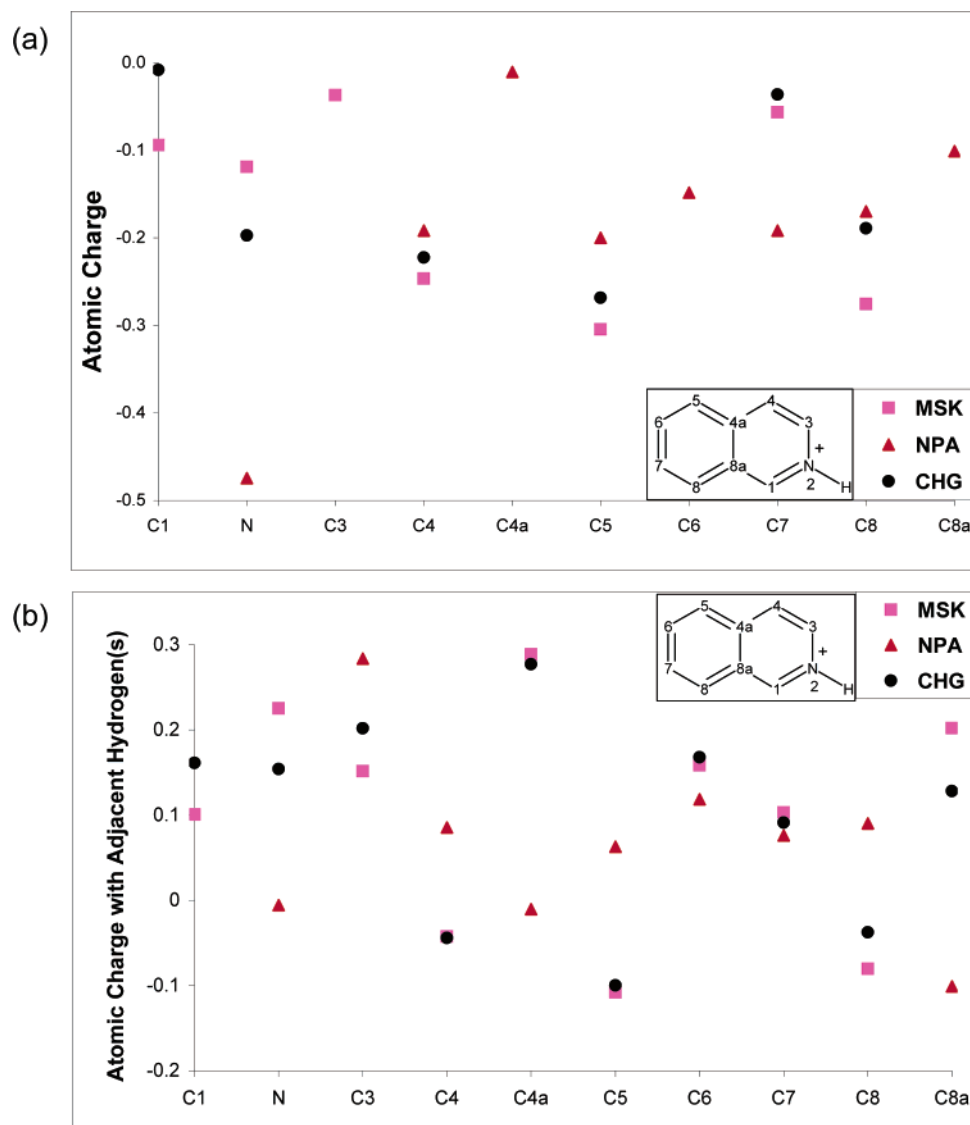


**Figure 3.** Atomic charges (condensed electrostatic potential) of *protonated* isoquinoline.

reaction at carbon 6 and carbon 8.<sup>42</sup> It seems reasonable to infer that carbon 6 and carbon 8 are the most reactive positions, with carbon 8 being slightly more reactive, at least for some electrophiles. If one increases the temperature and the amount of reagent, then one can add another chlorine to 10-hydroxy-10,9-borazarophenanthrene; forming the 2,6,8-trisubstituted product.<sup>41</sup> Carbon 2 is essentially unreactive with respect to nitration and bromination, however.<sup>41,42</sup> We infer, then, that the experimental reactivity profile can be summarized as

$$C8 \approx C6 \gg C2 \quad (10)$$

Theoretical electronic-structure treatments suggest that carbon 4 and carbon 2 should have similar reactivities. It is known, however, that steric congestion significantly reduces the rate of reaction at carbon 4.<sup>43</sup>

One might expect that, like isoquinoline, 10-R-10,9-borazarophenanthrene would be protonated. This is not the case. First of all, note that the nitrogen atom in 10,9-borazarophenanthrene already has four bonds, which reduces its susceptibility to protonation. Second, the presence of the

adjacent boron atom (which accepts electrons from the p orbital of the  $sp^2$  hybridized nitrogen atom) reduces the basicity of the nitrogen. Protonation does occur, but only when the compound is heated in concentrated sulfuric acid.<sup>40,44</sup> (Upon protonation in that environment, the central ring breaks and boron is lost.) Under any reasonable set of experimental conditions, then, 10-R-10,9-borazarophenanthrene is not protonated.

**2. Frontier Molecular Orbitals, Condensed Fukui Functions, and Atomic Charges.** Frontier molecular orbital theory does not predict the reactivity in these molecules. According to FMO, carbon 2 is slightly more reactive than carbon 4, which is slightly more reactive than the bond between carbon 6 and carbon 7.<sup>14</sup> (Both carbon 6 and carbon 7 have substantial contributions from the HOMO orbital.) There is very little frontier molecular orbital density on carbon 8.

The condensed Fukui functions for 10-hydroxy-10,9-borazarophenanthrene ( $R = OH$ ) are reported in Figures 6b and 7b. The condensed Fukui function gives results that are more in line with the experiment than frontier molecular

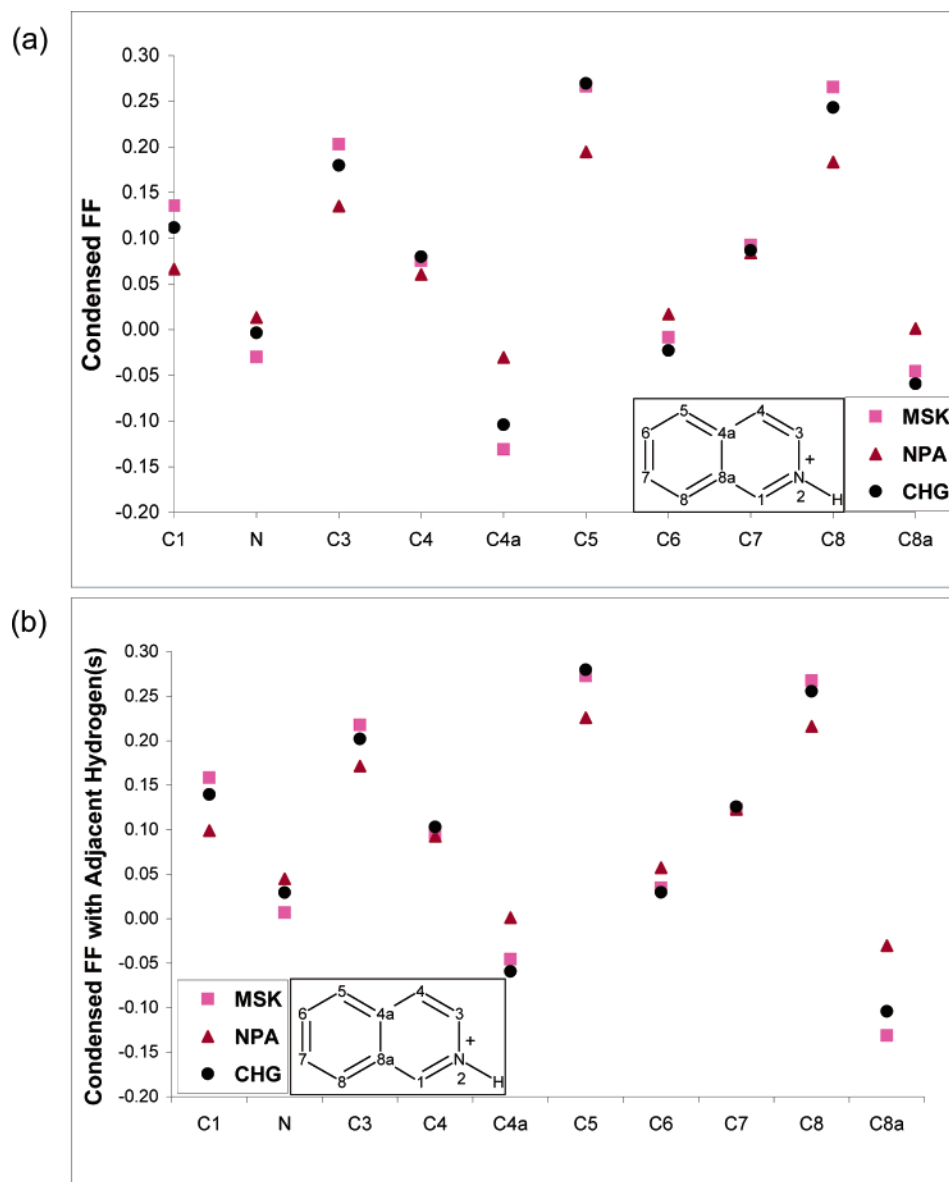
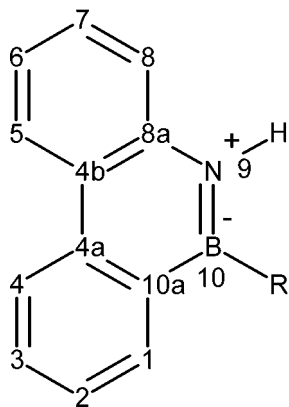


**Figure 4.** Condensed Fukui function of protonated isoquinoline. In a, we compute the Fukui function from the difference of atomic charges. In b, we add to each indicated atom the condensed Fukui functions of the hydrogen atoms bonded to it. The atomic numbering scheme is included as an inset. Experimentally, C5 is the most reactive, followed by C8. C4 is unreactive.



orbital theory. In particular, the Fukui function predicts that carbon 6 is the most reactive position in the molecule. Carbon 2 and carbon 4b are the next most reactive positions, followed by carbon 4. The Fukui function predicts that carbon 8 is essentially unreactive. The predicted reactivity at carbon 4b

demonstrates a recurrent feature in electrophilic polyaromatic substitution reactions. Qualitative reactivity indicators often predict ipso addition of electrophiles to polyaromatic compounds, but in many cases, ipso addition is a mechanistic dead end: although it is sometimes the most favorable orientation for the reactants, the barrier separating the ipso reactive intermediate from stable product molecules is very high. For example, because there are no hydrogen atoms at carbon 4b, electrophilic aromatic substitution cannot occur. Consequently, addition at carbon 4b requires a loss of aromaticity.

The atomic charges are reported in Figures 6a and 7a. Though carbon 10a, nitrogen, and oxygen are all negatively charged, these sites are not susceptible to electrophilic aromatic substitution. While a positively charged electrophile might form an “ion-pair” association complex with one of these sites, no further reaction at these sites is possible under ordinary conditions. For carbon 10a, there is no hydrogen

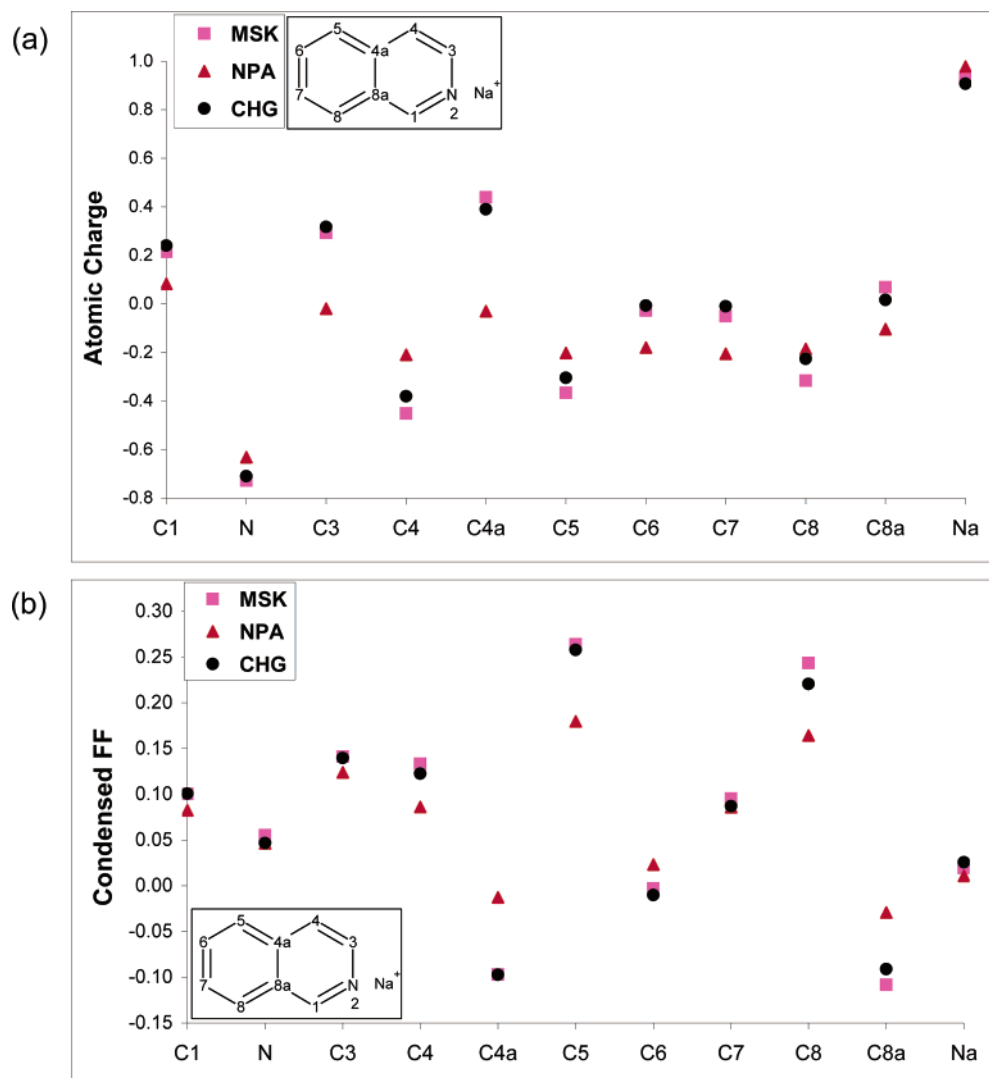


**Figure 5.** (a) Atomic charges and (b) condensed Fukui functions of isoquinoline with a sodium “spectator cation.” Qualitatively, the plot with hydrogens summed into adjacent carbons is very similar.

atom to serve as a leaving group. While there is a hydrogen bound to the nitrogen atom, bonds between hydrogen and electron-deficient  $sp^2$  hybridized nitrogen atoms are very strong, so this hydrogen atom is a poor leaving group.<sup>45</sup> Oxygen–hydrogen bonds are generally stronger than carbon–hydrogen bonds, so the hydrogen atom bonded to oxygen is also a poor leaving group. Consequently, we expect the chemistry at C10a, nitrogen, and oxygen is limited to the formation and dissociation of weak “ion-pairing”-type interactions.

Among sites that are susceptible to electrophilic aromatic substitution, carbon 8 is the most negatively charged, with carbon 6 and carbon 4 having somewhat smaller, but still substantial, negative charges. Carbon 2 is also negatively charged.

We predict, then, that carbon 8 and carbon 6 are the most highly reactive sites on the basis of electrostatic effects and electron-transfer effects, respectively. Carbon 2 and carbon 4 represent tradeoffs: these molecular sites have reasonably large Fukui functions and reasonably negative charges. If the reactivity of 10-hydroxy-10,9-borazarophenanthrene was strongly electrostatically controlled, then carbon 6 should

be less reactive because large values for the Fukui function are unfavorable in that situation. Similarly, if the reactivity was strongly electron-transfer-controlled, then carbon 8 should be less reactive because small values of the electrostatic potential are unfavorable in that situation. Both carbon 8 and carbon 6 are observed to be reactive, so the reactivity must be jointly controlled by electrostatic and electron-transfer effects.

Because MSK and CHG charges are both designed to reproduce the electrostatic potential, these two choices of charges should resemble one another and, hopefully, also the charges derived from NPA. Examining Figure 7, it seems that the agreement between the different population analysis schemes is slightly better if the charges on the heavy atoms are combined with the charges on their adjacent hydrogen atoms. We will base the rest of our analysis on the plots with the hydrogen atoms summed in; because of the similarity between the results in Figures 6 and 7, this will not affect our results very much. Indeed, the main trends in the values of the charges and the condensed Fukui functions seem to be reproduced no matter which population analysis scheme is being employed. This is reassuring, because there



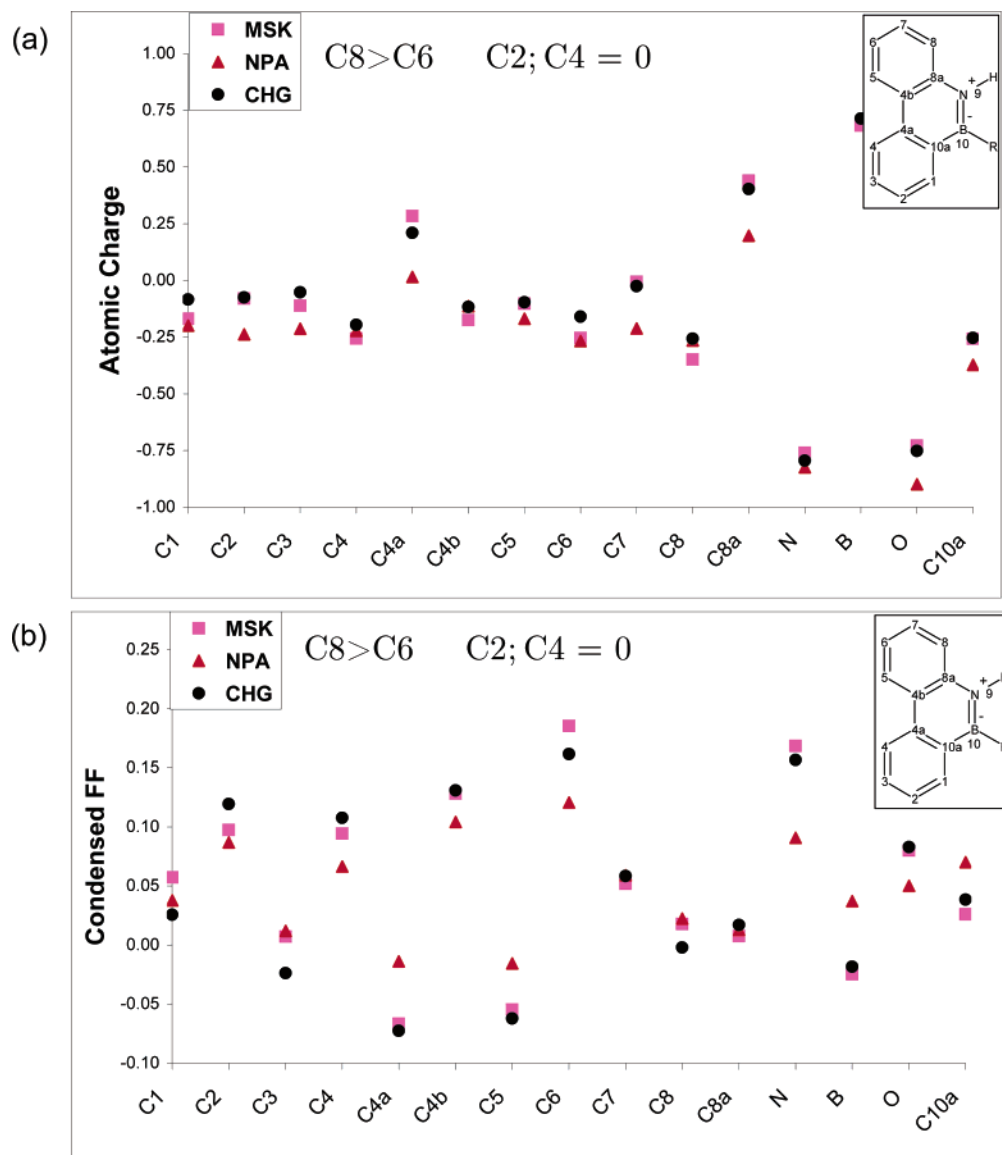


**Figure 6.** (a) Atomic charges and (b) condensed Fukui functions of 10-hydroxy-10,9-borazarophenanthrene. The atomic numbering scheme is included as an inset. Experimentally, C8 is the most reactive, followed by C6 and then C2. Other sites are unreactive.

is no a priori reason to assert the superiority of any one of the population analysis schemes.<sup>46</sup>

**3. Application of the Condensed General-Purpose Reactivity Indicator.** Because 10-hydroxy-10,9-borazarophenanthrene is a case of joint electrostatic and electron-transfer control, it seems to be a suitable test for the general-purpose reactivity indicator developed in the previous paper.<sup>1</sup> It is difficult to distill the immense amount of information in this indicator

$$\Xi_{\Delta N \leq 0, \alpha}^{\kappa} = (\kappa + 1)q_{\text{nucleophile}, \alpha}^{(0)} - \Delta N(\kappa - 1)f_{\text{nucleophile}, \alpha}^{-} \quad (11)$$

into an easily digestible form, however. Recall that  $\Xi_{\Delta N, \alpha}^{\kappa}$  depends on two parameters:  $\kappa$ , which measures the relative importance of electrostatic control ( $\kappa \approx 1$ ) and electron-transfer control ( $\kappa \approx -1$ ), and  $\Delta N$ , which measures the amount of electron transfer.  $\Xi_{\Delta N, \alpha}^{\kappa}$  is a bivariate function for every atom in the system! What we really want to know is which site is most reactive and how (and whether) the choice

of reaction site changes as a result of changing electrophilic reagents and reaction conditions. We have found that the key information about the reactivity of the molecule can be summarized using what we term “reactivity transition tables” (see Tables 1–4). To make a reactivity transition table, one starts by computing the value of  $\Xi_{\Delta N \leq 0, \alpha}^{\kappa}$  for every atom in the molecule and for the entire chemically relevant range of choices for the amount of electron transfer ( $-1 \leq \Delta N \leq 0$ ) and the extent of electrostatic/electron-transfer control ( $\kappa$ ). As established in the previous section, electrophilic attack on 10-hydroxy-10,9-borazarophenanthrene is jointly controlled by electrostatic and electron-transfer effects, so we consider only  $-1 \leq \kappa \leq 1$ . In constructing the reactivity transition tables, we restrict ourselves to carbons that are susceptible to electrophilic aromatic substitution.

One determines which atom is the most reactive by locating the atom with the smallest value of  $\Xi_{\Delta N \leq 0, \alpha}^{\kappa}$ . We insert this value in the “first choice” reactivity transition table and then color-code the cell so that it is clear which carbon

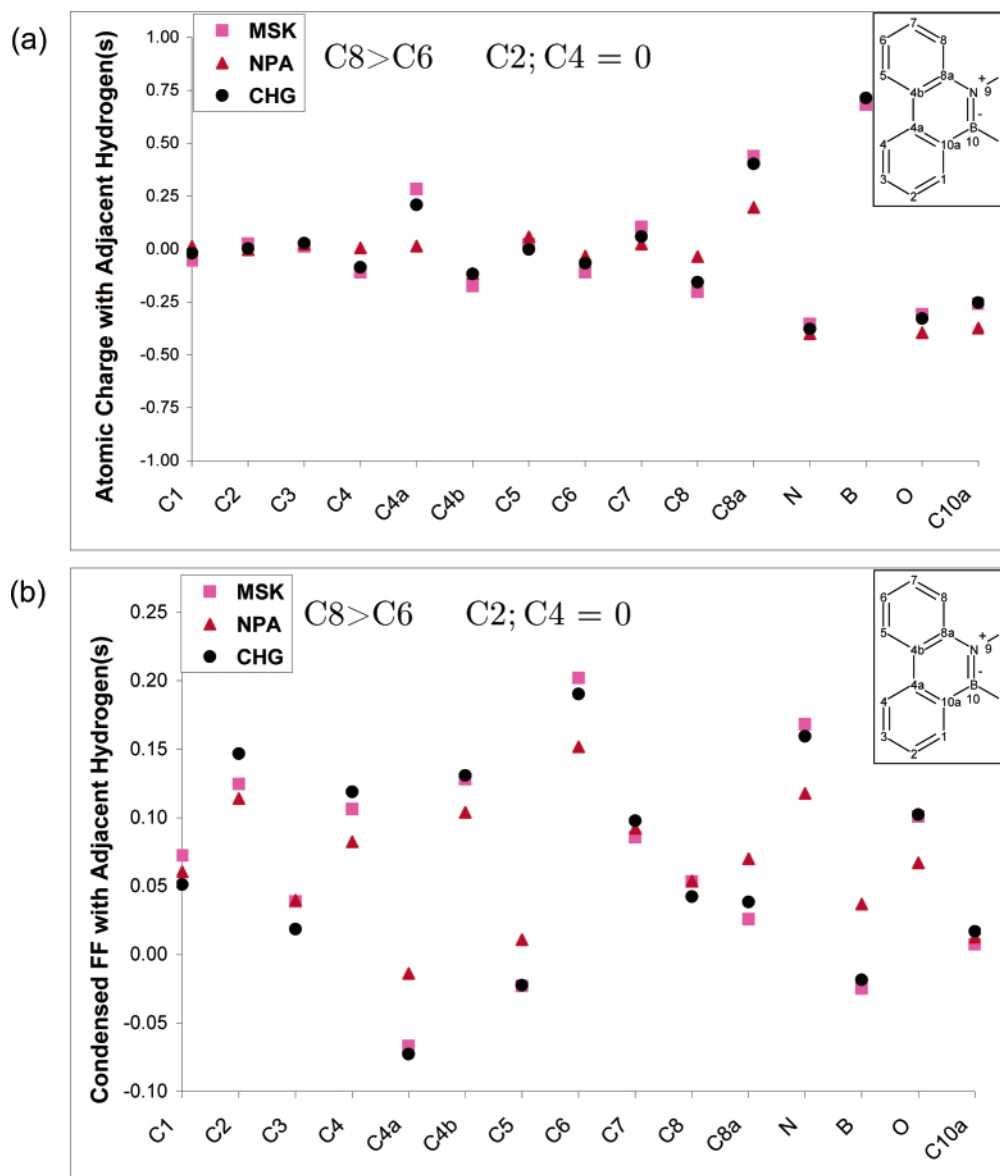


**Figure 7.** (a) “Hydrogen-summed” atomic charges and (b) “hydrogen-summed” condensed Fukui functions of 10-hydroxy-10,9-borazarophenanthrene. Unlike Figure 6, the reactivity indicators for hydrogen atoms have been added to the reactivity indicators of the heavy atoms to which they are bonded.

is reacting. The second most reactive atom is the one with the second smallest value for  $\Xi_{\Delta N \leq 0, \alpha}^{\kappa}$ . We insert this value in the “second choice” reactivity transition table and color-code the cells to indicate the second most reactive carbon. If the difference between the values of  $\Xi_{\Delta N \leq 0, \alpha}^{\kappa}$  for the first and second choices is relatively small, then, one expects that both possible product molecules will form. If the difference between the “first choice” and “second choice” values of  $\Xi_{\Delta N \leq 0, \alpha}^{\kappa}$  is relatively large, vigorous reaction conditions may be required to form the secondary product.

Reactivity transition tables contain both qualitative and quantitative data on reactivity. At a quantitative level, the “first choice” and “second choice” reactivity transition tables give information about the relative favorability of the primary and secondary products. At a qualitative level, the reactivity transition table can be read as a “phase diagram” for chemical reactivity. Examine Table 1a. When the nucleophile reacts with a very hard electrophile (so that the reaction is mostly

electrostatically controlled and  $\kappa \approx 1$ ), reactions occur at carbon 8. As the electrophile becomes softer and the extent of electron transfer increases, carbon 6 becomes the preferred site for reactivity. In the “transition region” between carbon 8 and carbon 6, one would expect a mixture of products. In this way, a reactivity transition table contains information about how to choose the electrophile so that a desired product is formed.

Reactivity transition tables for different types of population analyses are provided in Table 1 (NPA), Table 2 (MSK), and Table 3 (CHelpG). In each case, carbon 8 is the most favorable site when electrostatic effects are dominant ( $\kappa \approx 1$  and  $\Delta N \approx 0$ ) and carbon 6 is the most favorable site when electron-transfer effects are dominant ( $\kappa \approx -1$  and  $\Delta N \approx -1$ ). Experimental results indicate that the chlorination and nitration of 10-hydroxy-10,9-borazarophenanthrene occur on carbon 8 and carbon 6, with a small preference for carbon 8. In these reactions, the electrophile is reasonably hard, and

**Table 1.** Reactivity Transition Tables for 10-Hydroxy-10,9-borazarophenanthrene Using Natural Population Analysis for the Charges and Fukui Functions on Hydrogens Summed into the Adjacent Heavy Atoms<sup>a</sup>

(a)

<i>N</i>	<i>K</i>										
	1.0	0.8	0.6	0.4	0.2	0	-0.2	-0.4	-0.6	-0.8	-1.0
-1.0	-0.072	-0.090	-0.113	-0.137	-0.161	-0.185	-0.208	-0.232	-0.256	-0.280	-0.303
-0.9	-0.072	-0.086	-0.107	-0.128	-0.149	-0.169	-0.190	-0.211	-0.232	-0.252	-0.273
-0.8	-0.072	-0.083	-0.101	-0.119	-0.137	-0.154	-0.172	-0.190	-0.207	-0.225	-0.243
-0.7	-0.072	-0.080	-0.095	-0.110	-0.124	-0.139	-0.154	-0.168	-0.183	-0.198	-0.212
-0.6	-0.072	-0.077	-0.089	-0.101	-0.112	-0.124	-0.136	-0.147	-0.159	-0.170	-0.182
-0.5	-0.072	-0.074	-0.083	-0.092	-0.100	-0.109	-0.117	-0.126	-0.135	-0.143	-0.152
-0.4	-0.072	-0.071	-0.077	-0.082	-0.088	-0.094	-0.099	-0.105	-0.110	-0.116	-0.121
-0.3	-0.072	-0.068	-0.071	-0.073	-0.076	-0.078	-0.081	-0.083	-0.086	-0.088	-0.091
-0.2	-0.072	-0.067	-0.065	-0.064	-0.064	-0.063	-0.063	-0.062	-0.062	-0.061	-0.061
-0.1	-0.072	-0.066	-0.060	-0.055	-0.052	-0.048	-0.045	-0.041	-0.037	-0.034	-0.030
0.0	-0.072	-0.065	-0.058	-0.051	-0.043	-0.036	-0.029	-0.022	-0.014	-0.007	
	Carbon 2		Carbon 4			Carbon 6			Carbon 8		

(b)

<i>N</i>	<i>K</i>										
	1.0	0.8	0.6	0.4	0.2	0	-0.2	-0.4	-0.6	-0.8	-1.0
-1.0	-0.066	-0.076	-0.079	-0.083	-0.095	-0.117	-0.139	-0.161	-0.184	-0.206	-0.228
-0.9	-0.066	-0.075	-0.077	-0.080	-0.086	-0.106	-0.125	-0.145	-0.165	-0.185	-0.205
-0.8	-0.066	-0.074	-0.075	-0.076	-0.078	-0.094	-0.112	-0.129	-0.147	-0.165	-0.182
-0.7	-0.066	-0.073	-0.073	-0.073	-0.073	-0.083	-0.098	-0.113	-0.129	-0.144	-0.160
-0.6	-0.066	-0.071	-0.071	-0.070	-0.069	-0.071	-0.084	-0.098	-0.111	-0.124	-0.137
-0.5	-0.066	-0.070	-0.069	-0.067	-0.065	-0.063	-0.071	-0.082	-0.092	-0.103	-0.114
-0.4	-0.066	-0.069	-0.066	-0.063	-0.061	-0.058	-0.057	-0.066	-0.074	-0.083	-0.091
-0.3	-0.066	-0.068	-0.064	-0.060	-0.056	-0.052	-0.048	-0.050	-0.056	-0.062	-0.068
-0.2	-0.066	-0.065	-0.062	-0.057	-0.052	-0.047	-0.042	-0.037	-0.038	-0.042	-0.046
-0.1	-0.066	-0.062	-0.059	-0.054	-0.048	-0.041	-0.035	-0.029	-0.023	-0.021	-0.023
0.0	-0.066	-0.059	-0.053	-0.046	-0.039	-0.033	-0.026	-0.020	-0.013	-0.007	
	Carbon 2		Carbon 4			Carbon 6			Carbon 8		

<sup>a</sup> (Part a) First choice: the minimum values of  $\Xi_{\Delta N \leq 0}^K$  denote where the molecule is most reactive. (Part b) Second choice: the second-smallest values for  $\Xi_{\Delta N \leq 0}^K$ , denoting the second most reactive carbon.

**Table 2.** Reactivity Transition Tables for 10-Hydroxy-10,9-borazarophenanthrene Using CHelpG Population Analysis with the Charges and Fukui Functions on Hydrogens Summed into the Adjacent Heavy Atoms<sup>a</sup>

(a)

<i>N</i>	<i>K</i>										
	1.0	0.8	0.6	0.4	0.2	0	-0.2	-0.4	-0.6	-0.8	-1.0
-1.0	-0.312	-0.289	-0.267	-0.244	-0.233	-0.257	-0.282	-0.307	-0.331	-0.356	-0.381
-0.9	-0.312	-0.289	-0.265	-0.241	-0.218	-0.238	-0.259	-0.280	-0.301	-0.322	-0.343
-0.8	-0.312	-0.288	-0.263	-0.239	-0.214	-0.219	-0.236	-0.253	-0.270	-0.288	-0.305
-0.7	-0.312	-0.287	-0.262	-0.236	-0.211	-0.200	-0.214	-0.227	-0.240	-0.253	-0.266
-0.6	-0.312	-0.286	-0.260	-0.234	-0.208	-0.181	-0.191	-0.200	-0.210	-0.219	-0.228
-0.5	-0.312	-0.285	-0.258	-0.231	-0.204	-0.177	-0.168	-0.173	-0.179	-0.185	-0.190
-0.4	-0.312	-0.284	-0.257	-0.229	-0.201	-0.173	-0.145	-0.147	-0.149	-0.150	-0.152
-0.3	-0.312	-0.284	-0.255	-0.226	-0.197	-0.169	-0.140	-0.120	-0.118	-0.116	-0.114
-0.2	-0.312	-0.283	-0.253	-0.224	-0.194	-0.165	-0.135	-0.105	-0.088	-0.082	-0.076
-0.1	-0.312	-0.282	-0.251	-0.221	-0.191	-0.160	-0.130	-0.100	-0.069	-0.048	-0.038
0.0	-0.312	-0.281	-0.250	-0.219	-0.187	-0.156	-0.125	-0.094	-0.062	-0.031	
	Carbon 2		Carbon 4			Carbon 6			Carbon 8		

(b)

<i>N</i>	<i>K</i>										
	1.0	0.8	0.6	0.4	0.2	0	-0.2	-0.4	-0.6	-0.8	-1.0
-1.0	-0.174	-0.180	-0.187	-0.208	-0.221	-0.206	-0.212	-0.219	-0.234	-0.264	-0.294
-0.9	-0.174	-0.178	-0.182	-0.197	-0.218	-0.194	-0.198	-0.202	-0.211	-0.237	-0.264
-0.8	-0.174	-0.176	-0.177	-0.185	-0.202	-0.190	-0.184	-0.185	-0.187	-0.211	-0.235
-0.7	-0.174	-0.173	-0.173	-0.174	-0.187	-0.186	-0.170	-0.169	-0.168	-0.185	-0.206
-0.6	-0.174	-0.171	-0.168	-0.165	-0.172	-0.181	-0.155	-0.152	-0.149	-0.158	-0.176
-0.5	-0.174	-0.169	-0.163	-0.158	-0.157	-0.162	-0.150	-0.135	-0.130	-0.132	-0.147
-0.4	-0.174	-0.166	-0.158	-0.150	-0.143	-0.143	-0.145	-0.119	-0.111	-0.105	-0.117
-0.3	-0.174	-0.164	-0.154	-0.143	-0.133	-0.124	-0.122	-0.111	-0.092	-0.082	-0.088
-0.2	-0.174	-0.161	-0.149	-0.136	-0.123	-0.111	-0.099	-0.094	-0.076	-0.060	-0.059
-0.1	-0.174	-0.159	-0.144	-0.129	-0.114	-0.099	-0.084	-0.069	-0.057	-0.039	-0.029
0.0	-0.174	-0.157	-0.139	-0.122	-0.104	-0.087	-0.070	-0.052	-0.035	-0.017	
	Carbon 2		Carbon 4			Carbon 6			Carbon 8		

<sup>a</sup> (Part a) First choice: the minimum values of  $\Xi_{\Delta N \leq 0}^K$  denote where the molecule is most reactive. (Part b) Second choice: the second-smallest values for  $\Xi_{\Delta N \leq 0}^K$ , denoting the second most reactive carbon.

so the reaction is probably more electrostatically controlled than it is electron-transfer-controlled ( $0 < \kappa < 1$ ). Electron transfer to the electrophile will be important, but incomplete ( $\Delta N \approx -0.5$ ). In Tables 2a and 3a (on the basis of CHelpG and MSK population analysis, with the hydrogenic contribu-

tions summed into the adjacent heavy atoms), these experimental conditions place one near the transition region between carbon 8 and carbon 6, but in regions where carbon 8 would be predicted to be slightly more reactive. In Table 1a (on the basis of natural population analysis), this places

**Table 3.** Reactivity Transition Tables for 10-Hydroxy-10,9-borazarophenanthrene Using Merz–Singh–Kollman Population Analysis with the Charges and Fukui Functions on Hydrogens Summed into the Adjacent Heavy Atoms<sup>a</sup>

(a)

<i>N</i>	<i>K</i>										
	1.0	0.8	0.6	0.4	0.2	0	-0.2	-0.4	-0.6	-0.8	-1.0
-1.0	-0.697	-0.631	-0.565	-0.499	-0.453	-0.439	-0.426	-0.412	-0.398	-0.385	-0.371
-0.9	-0.697	-0.631	-0.564	-0.498	-0.438	-0.421	-0.404	-0.386	-0.369	-0.351	-0.334
-0.8	-0.697	-0.630	-0.563	-0.497	-0.430	-0.402	-0.381	-0.360	-0.339	-0.318	-0.297
-0.7	-0.697	-0.630	-0.563	-0.496	-0.428	-0.384	-0.359	-0.334	-0.309	-0.284	-0.260
-0.6	-0.697	-0.630	-0.562	-0.494	-0.427	-0.365	-0.337	-0.308	-0.280	-0.251	-0.223
-0.5	-0.697	-0.629	-0.561	-0.493	-0.425	-0.358	-0.314	-0.282	-0.250	-0.218	-0.185
-0.4	-0.697	-0.629	-0.561	-0.492	-0.424	-0.356	-0.292	-0.256	-0.220	-0.184	-0.148
-0.3	-0.697	-0.629	-0.560	-0.491	-0.423	-0.354	-0.285	-0.230	-0.191	-0.151	-0.111
-0.2	-0.697	-0.628	-0.559	-0.490	-0.421	-0.352	-0.283	-0.214	-0.161	-0.118	-0.074
-0.1	-0.697	-0.628	-0.558	-0.489	-0.420	-0.350	-0.281	-0.212	-0.142	-0.084	-0.037
0.0	-0.697	-0.627	-0.558	-0.488	-0.418	-0.349	-0.279	-0.209	-0.139	-0.070	
	Carbon 2		Carbon 4			Carbon 6			Carbon 8		

(b)

<i>N</i>	<i>K</i>										
	1.0	0.8	0.6	0.4	0.2	0	-0.2	-0.4	-0.6	-0.8	-1.0
-1.0	-0.513	-0.494	-0.481	-0.467	-0.433	-0.366	-0.318	-0.286	-0.254	-0.221	-0.194
-0.9	-0.513	-0.491	-0.473	-0.456	-0.431	-0.365	-0.307	-0.273	-0.238	-0.204	-0.175
-0.8	-0.513	-0.487	-0.466	-0.445	-0.424	-0.363	-0.296	-0.260	-0.223	-0.187	-0.156
-0.7	-0.513	-0.483	-0.458	-0.433	-0.409	-0.361	-0.294	-0.246	-0.208	-0.170	-0.136
-0.6	-0.513	-0.479	-0.451	-0.422	-0.394	-0.359	-0.292	-0.233	-0.193	-0.153	-0.117
-0.5	-0.513	-0.476	-0.443	-0.411	-0.379	-0.347	-0.290	-0.222	-0.178	-0.136	-0.097
-0.4	-0.513	-0.472	-0.436	-0.400	-0.364	-0.328	-0.287	-0.219	-0.163	-0.119	-0.078
-0.3	-0.513	-0.468	-0.429	-0.389	-0.349	-0.310	-0.270	-0.217	-0.148	-0.102	-0.058
-0.2	-0.513	-0.466	-0.421	-0.378	-0.334	-0.291	-0.248	-0.204	-0.145	-0.085	-0.039
-0.1	-0.513	-0.464	-0.414	-0.367	-0.320	-0.273	-0.225	-0.178	-0.131	-0.073	-0.019
0.0	-0.513	-0.462	-0.411	-0.359	-0.308	-0.257	-0.205	-0.154	-0.103	-0.051	
	Carbon 2		Carbon 4			Carbon 6			Carbon 8		

<sup>a</sup> (Part a) First choice: the minimum values of  $\Xi_{\Delta N \leq 0}^K$  denote where the molecule is most reactive. (Part b) Second choice: the second smallest values for  $\Xi_{\Delta N \leq 0}^K$ , denoting the second most reactive carbon.

**Table 4.** Reactivity Transition Tables for 10-Methyl-10,9-borazarophenanthrene Using Natural Population Analysis with the Charges and Fukui Functions on Hydrogens Summed into the Adjacent Heavy Atoms<sup>a</sup>

(a)

<i>N</i>	<i>K</i>										
	1.0	0.8	0.6	0.4	0.2	0	-0.2	-0.4	-0.6	-0.8	-1.0
-1.0	-0.067	-0.066	-0.074	-0.094	-0.115	-0.135	-0.159	-0.183	-0.207	-0.232	-0.256
-0.9	-0.067	-0.066	-0.069	-0.087	-0.105	-0.123	-0.143	-0.165	-0.187	-0.209	-0.231
-0.8	-0.067	-0.065	-0.065	-0.080	-0.096	-0.112	-0.128	-0.147	-0.166	-0.186	-0.205
-0.7	-0.067	-0.064	-0.062	-0.073	-0.086	-0.100	-0.113	-0.129	-0.146	-0.163	-0.179
-0.6	-0.067	-0.064	-0.061	-0.066	-0.077	-0.088	-0.099	-0.111	-0.125	-0.140	-0.154
-0.5	-0.067	-0.063	-0.059	-0.059	-0.067	-0.076	-0.084	-0.093	-0.105	-0.117	-0.128
-0.4	-0.067	-0.063	-0.058	-0.054	-0.058	-0.064	-0.070	-0.076	-0.084	-0.093	-0.102
-0.3	-0.067	-0.062	-0.057	-0.052	-0.048	-0.052	-0.056	-0.060	-0.064	-0.070	-0.077
-0.2	-0.067	-0.061	-0.056	-0.050	-0.045	-0.040	-0.042	-0.043	-0.045	-0.047	-0.051
-0.1	-0.067	-0.061	-0.055	-0.049	-0.043	-0.036	-0.030	-0.027	-0.026	-0.025	-0.026
0.0	-0.067	-0.060	-0.054	-0.047	-0.040	-0.033	-0.027	-0.020	-0.013	-0.007	
	Carbon 2		Carbon 4			Carbon 6			Carbon 8		

(b)

<i>N</i>	<i>K</i>										
	1.0	0.8	0.6	0.4	0.2	0	-0.2	-0.4	-0.6	-0.8	-1.0
-1.0	-0.033	-0.054	-0.065	-0.086	-0.110	-0.134	-0.156	-0.176	-0.196	-0.217	-0.237
-0.9	-0.033	-0.051	-0.064	-0.078	-0.100	-0.122	-0.141	-0.159	-0.177	-0.195	-0.213
-0.8	-0.033	-0.049	-0.063	-0.070	-0.089	-0.109	-0.127	-0.143	-0.158	-0.174	-0.190
-0.7	-0.033	-0.047	-0.060	-0.063	-0.079	-0.096	-0.113	-0.126	-0.140	-0.153	-0.166
-0.6	-0.033	-0.044	-0.055	-0.057	-0.069	-0.083	-0.097	-0.110	-0.121	-0.131	-0.142
-0.5	-0.033	-0.042	-0.050	-0.056	-0.059	-0.070	-0.082	-0.093	-0.102	-0.110	-0.119
-0.4	-0.033	-0.039	-0.046	-0.052	-0.050	-0.057	-0.066	-0.075	-0.083	-0.089	-0.095
-0.3	-0.033	-0.037	-0.041	-0.045	-0.047	-0.045	-0.051	-0.058	-0.064	-0.067	-0.071
-0.2	-0.033	-0.035	-0.036	-0.038	-0.039	-0.039	-0.036	-0.040	-0.043	-0.046	-0.047
-0.1	-0.033	-0.032	-0.031	-0.030	-0.029	-0.029	-0.028	-0.024	-0.023	-0.024	-0.024
0.0	-0.033	-0.030	-0.027	-0.023	-0.020	-0.017	-0.013	-0.010	-0.007	-0.003	
	Carbon 2		Carbon 4			Carbon 6			Carbon 8		

<sup>a</sup> (Part a) First choice: the minimum values of  $\Xi_{\Delta N \leq 0}^K$  denote where the molecule is most reactive. (Part b) Second choice: the second smallest values for  $\Xi_{\Delta N \leq 0}^K$ , denoting the second most reactive carbon.

one in the region where carbon 6 is the most favorable, though one is still reasonably close to the region where carbon 8 would be favored.

Examining the second-choice reactivity transition diagrams in Tables 1b (NPA), 2b (ChelpG), and 3b (MSK), one finds that carbon 4 and carbon 2 are also predicted to be reactive.



Carbon 4 would be predicted to be more reactive than carbon 2 except when electron-transfer effects are dominant ( $\kappa \approx -1$ ). Experimentally, carbon 4 is much less reactive than one would expect on the basis of electronic-structure considerations alone. Dewar noted this effect as early as 1956 and suggested that the abnormally low reactivity of carbon 4 is due to steric effects, rather than electronic structure considerations.<sup>43</sup> Our indicator does not include any information about steric hindrance, so it is not surprising that it also overestimates the reactivity of carbon 4. Examining the values of  $\Xi_{\Delta N \leq 0, \alpha}^{\kappa}$  where carbon 4 emerges as the “second choice” reactivity site, we observe that there is a large gap between the predicted reactivity of carbon 4 and the reactivity of the most reactive site.<sup>47</sup> This indicates that, whenever carbon 4 is the “second choice” reactive site, the “first choice” reactive site is much more reactive. When the second-choice reactive site is much less favorable than the first-choice reactive site, one expects that the secondary product will be a very small percentage of the total yield and, thus, difficult to isolate and characterize.

The overall picture that emerges is fairly convincing: carbon 6 and carbon 8 are the most reactive, with the population analysis schemes based on electrostatic fitting successfully predicting that carbon 8 should be slightly more reactive. Carbon 2 is predicted to be much less reactive, which agrees with the experimental observation that reactions at carbon 2 only occur under very special conditions: chlorination at high temperatures with excess chlorine.<sup>41</sup>

Our analysis also indicates that, under the appropriate conditions, carbon 6 should be more reactive than carbon 8. Indeed, Friedel–Crafts acetylation of 10-hydroxy-10,9-borazarophenanthrene occurs predominately at carbon 6, with the diacetylated product corresponding to reaction at both carbon 6 and carbon 8 as a secondary product.<sup>44</sup> The monoacetylated product corresponding to reaction at carbon 8 is not observed. Dewar explained this by hypothesizing that the nitrogen atom is complexed by the  $\text{AlCl}_3$  catalyst, which might make carbon 8 sterically inaccessible.<sup>44,48</sup> Our analysis suggests another possibility, however. The mechanism of Friedel–Crafts acetylation involves the addition of the resonance-stabilized acetyl carbocation ( $\text{CH}_3\text{CO}^+$ ) to the aromatic ring. Because this is a carbocation, we expect that  $\Delta N \approx -1$ . Moreover, this carbocation is resonance-stabilized and, additionally, might be somewhat stabilized by complexation of the catalyst. As such, the charge on the electrophilic carbon atom is relatively small, and moreover, we expect that the acetyl carbocation is relatively soft. Accordingly, we expect that the reaction will be mostly electron-transfer-controlled,  $-1 < \kappa < 0$ . Referring to Tables 1a–3a, one finds that, under these conditions, carbon 6 is more reactive than any of the other molecular sites.

To this point, we have focused on hydroxylated 10,9-borazarophenanthrene ( $\text{R} = \text{OH}$ ) rather than on the methylated compound. For the hydroxylated compound, the various population analysis schemes gave qualitatively similar results. This was not true for  $\text{R} = \text{CH}_3$ , and summing the charges of the hydrogen atoms into the adjacent heavy atoms did not substantially improve the agreement between the various population analysis schemes. Indeed, even though

the MSK and CHelpG charges are both based on fitting the electrostatic potential, the results from these population analysis schemes were significantly different for  $\text{R} = \text{CH}_3$ . This can be contrasted with the favorable results in Figure 7a, where the different electrostatic potential fitting methods gave substantially similar results. Given the unreliability of our charges when  $\text{R} = \text{CH}_3$ , we have chosen to focus our discussion on the hydroxylated compound. Nonetheless, the main results for  $\text{R} = \text{CH}_3$  are broadly similar: carbon 6 and carbon 8 are ordinarily the most reactive, with carbon 4 and carbon 2 being less reactive. In many cases, carbon 4 is more reactive than carbon 2, and steric effects need to be invoked to describe the lack of reactivity at this site.<sup>43</sup> An exception occurs for the natural population analysis scheme, which is reported in Table 4a and b. In that case, carbon 8, carbon 6, and carbon 2 are all reasonably reactive, though carbon 8 and carbon 6 are likely to be the most reactive sites for chlorination and nitration.<sup>49</sup>

#### IV. Summary

To explore the validity of our methods, we studied three molecules where frontier molecular orbital theory fails to predict the correct reactivity. This analysis underscores, among other things, the importance of chemical reasoning when applying reactivity indicators. For example, while our results for isoquinoline were in stark disagreement with the experiment, isoquinoline is protonated under the experimental conditions. Adding a proton to isoquinoline brought our predictions into agreement with the experimental results. Similarly, when exploring electrophilic aromatic substitution on 10-R-10,9-borazarophenanthrenes, it was important to remember that “ipso” attack—attack on carbon atoms that do not have any adjacent hydrogen atoms—is a mechanistic dead end because there is no leaving group that the electrophile can “substitute” for.

The complex reactivity of 10-R-10,9-borazarophenanthrenes provided an ideal situation for testing the general-purpose reactivity indicator derived in the first paper of this series. Experimentally, chlorination, bromination, and nitration of 10-R-10,9-borazarophenanthrene occurs primarily on carbons 6 and 8 (with carbon 8 slightly favored). At higher temperatures, chlorination of 10-hydroxy-10,9-borazarophenanthrenes also gives some of the trichlorinated product, with the additional reaction occurring at carbon 2. Friedel–Crafts acetylation of 10-R-10,9-borazarophenanthrenes occurs primarily on carbon 6. Using the condensed version of our general-purpose reactivity indicator,  $\Xi_{\Delta N \leq 0, \alpha}^{\kappa}$ , we were able to explain these results: carbon 6 and carbon 8 are the most reactive sites, with carbon 8 favored for hard electrophiles; carbon 2 is significantly less reactive than carbon 6 and carbon 8 but is predicted to be more reactive than any other site except the sterically hindered carbon 4; because the acetyl carbocation is resonance-stabilized and a very good electron acceptor, the most reactive site should be carbon 6. To obtain these results, we used reactivity transition tables, which list the value of  $\Xi_{\Delta N \leq 0, \alpha}^{\kappa}$  at the most reactive (Tables 1a–4a) and second most-reactive (Tables 1b–4b) sites. The entries in the table are then color-coded according to the identity of the most reactive site. For molecules with multiple reactive



sites, reactivity transition tables provide a useful way of predicting how the regioselectivity of the molecule depends on the characteristics of the attacking reagent.

We are encouraged by these results. The new indicator,  $\Xi_{\Delta N}^K$ , coincides with conventional conceptual DFT reactivity indicators whenever they work but also provides theoretical insight and computational results that can be used to clarify situations where conventional reactivity indicators fail. Our future efforts in this area will focus on extending these results to other types of chemical reactions and refining the present indicator to account for the polarization of reactive sites.

**Acknowledgment.** Helpful discussions with Dr. David C. Thompson and Dr. Cherif Matta are acknowledged. NSERC, the Canada Research Chairs, and PREA provided funding for the Canadian authors. This research was performed when the second author visited McMaster University in the winter of 2005, and she wishes to thank the chemistry department at McMaster University for their hospitality.

## References

- (1) Anderson, J. S. M.; Melin, J.; Ayers, P. W. Conceptual Density-Functional Theory for General Chemical Reactions, Including Those That Are Neither Charge- nor Frontier-Orbital-Controlled. 1. Theory and Derivation of a General-Purpose Reactivity Indicator. *J. Chem. Theory Comput.* **2007**, *3*, 358–374.
- (2) Klopman, G. Chemical Reactivity and the Concept of Charge and Frontier-Controlled Reactions. *J. Am. Chem. Soc.* **1968**, *90*, 223–234.
- (3) Parr, R. G.; Pearson, R. G. Absolute Hardness: Companion Parameter to Absolute Electronegativity. *J. Am. Chem. Soc.* **1983**, *105* (26), 7512–7516.
- (4) Parr, R. G.; Donnelly, R. A.; Levy, M.; Palke, W. E. Electronegativity: The Density Functional Viewpoint. *J. Chem. Phys.* **1978**, *68* (8), 3801–3807.
- (5) Yang, W.; Mortier, W. J. The Use of Global and Local Molecular Parameters for the Analysis of the Gas-Phase Basicity of Amines. *J. Am. Chem. Soc.* **1986**, *108* (19), 5708–11.
- (6) Ayers, P. W.; Morrison, R. C.; Roy, R. K. Variational Principles for Describing Chemical Reactions: Condensed Reactivity Indices. *J. Chem. Phys.* **2002**, *116* (20), 8731–8744.
- (7) Langenaeker, W.; Demel, K.; Geerlings, P. Quantum-Chemical Study of the Fukui Function As a Reactivity Index. 2. Electrophilic Substitution on Mono-Substituted Benzenes. *THEOCHEM* **1991**, *80*, 329–342.
- (8) Meneses, L.; Tiznado, W.; Contreras, R.; Fuentealba, P. A Proposal for a New Local Hardness as Selectivity Index. *Chem. Phys. Lett.* **2004**, *383* (1–2), 181–187.
- (9) Martinez, A.; Vazquez, M. V.; Carreon-Macedo, J. L.; Sansores, L. E.; Salcedo, R. Benzene Fused Five-Membered Heterocycles. A Theoretical Approach. *Tetrahedron* **2003**, *59* (34), 6415–6422.
- (10) Ayers, P. W.; Levy, M. Perspective on “Density Functional Approach to the Frontier-Electron Theory of Chemical Reactivity” by Parr RG, Yang W (1984). *Theor. Chem. Acc.* **2000**, *103* (3–4), 353–360.
- (11) Yang, W.; Parr, R. G.; Pucci, R. Electron Density, Kohn–Sham Frontier Orbitals, and Fukui Functions. *J. Chem. Phys.* **1984**, *81* (6), 2862–2863.
- (12) Parr, R. G.; Yang, W. Density Functional Approach to the Frontier-Electron Theory of Chemical Reactivity. *J. Am. Chem. Soc.* **1984**, *106* (14), 4049–4050.
- (13) Melin, J.; Aparicio, F.; Subramanian, V.; Galvan, M.; Chattaraj, P. K. Is the Fukui Function a Right Descriptor of Hard–Hard Interactions? *J. Phys. Chem. A* **2004**, *108* (13), 2487–2491.
- (14) Dewar, M. J. S. A Critique of Frontier Orbital Theory. *THEOCHEM* **1989**, *59*, 301–23.
- (15) Frisch, M. J.; Trucks, G. W.; Schlegel, H. B.; Scuseria, G. E.; Robb, M. A.; Cheeseman, J. R.; Montgomery, J. A.; Vreven, T.; Kudin, K. N.; Burant, J. C.; Millam, J. M.; Iyengar, S. S.; Tomasi, J.; Barone, V.; Mennucci, B.; Cossi, M.; Scalmani, G.; Rega, N.; Peersson, G. A.; Nakatsuji, H.; Hada, M.; Ehara, M.; Toyota, K.; Fukuda, R.; Hasegawa, J.; Ishida, M.; Nakajima, T.; Honda, Y.; Kitao, O.; Nakai, H.; Klene, M.; Li, X.; Knox, J. E.; Hratchian, H. P.; Cross, J. B.; Adamo, C.; Jaramillo, J.; Gomperts, R.; Stratmann, R. E.; Yazyev, O.; Austin, A. J.; Cammi, R.; Pomelli, C.; Ochterski, J. W.; Ayala, P. Y.; Morokuma, K.; Voth, G. A.; Salvetti, O.; Dannenberg, J. J.; Zakrzewski, V. G.; Dapprich, S.; Daniels, A. D.; Strain, M. C.; Farkas, O.; Malick, D. K.; Rabuck, A. D.; Raghavachari, K.; Foresman, J. B.; Ortiz, J. V.; Cui, Q.; Baboul, A. G.; Clifford, S.; Cioslowski, J.; Stefanov, B. B.; Liu, G.; Liashenko, A.; Piskorz, P.; Komaromi, I.; Martin, R. L.; Fox, D. J.; Keith, T.; Al-Laham, M. A.; Peng, C. Y.; Nanayakkara, A.; Challacombe, M.; Gill, P. M. W.; Johnson, B.; Chen, W.; Wong, M. W.; Gonzalez, C.; Pople, J. A. *Gaussian 03*, revision C.02; Gaussian Inc.: Wallingford, CT, 2004.
- (16) Becke, A. D. Density-Functional Exchange-Energy Approximation With Correct Asymptotic-Behavior. *Phys. Rev. A: At., Mol., Opt. Phys.* **1988**, *38* (6), 3098–3100.
- (17) Becke, A. D. Density-Functional Thermochemistry. 3. The Role of Exact Exchange. *J. Chem. Phys.* **1993**, *98* (7), 5648–5652.
- (18) Lee, C.; Yang, W.; Parr, R. G. Development of the Colle-Salvetti Correlation-Energy Formula into a Functional of the Electron Density. *Phys. Rev. B: Condens. Matter Mater. Phys.* **1988**, *37* (2), 785–789.
- (19) Krishnan, R.; Binkley, J. S.; Seeger, R.; Pople, J. A. Self-Consistent Molecular-Orbital Methods. 20. Basis Set for Correlated Wave-Functions. *J. Chem. Phys.* **1980**, *72* (1), 650–654.
- (20) Mulliken, R. S. Electronic Population Analysis on LCAO-MO Molecular Wave Functions 1. *J. Chem. Phys.* **1955**, *23*, 1833.
- (21) Mulliken, R. S. Electronic Population Analysis on LCAO-MO Molecular Wave Functions 2. *J. Chem. Phys.* **1955**, *23*, 1841.
- (22) Mulliken, R. S. Electronic Population Analysis on LCAO-MO Molecular Wave Functions 4. *J. Chem. Phys.* **1955**, *23*, 2343.
- (23) Mulliken, R. S. Electronic Population Analysis on LCAO-MO Molecular Wave Functions 3. *J. Chem. Phys.* **1955**, *23*, 2338.
- (24) Reed, A. E.; Curtiss, L. A.; Weinhold, F. Intermolecular Interactions from a Natural Bond Orbital, Donor–Acceptor Viewpoint. *Chem. Rev.* **1988**, *88* (6), 899–926.

- (25) Reed, A. E.; Weinstock, R. B.; Weinhold, F. Natural-Population Analysis. *J. Chem. Phys.* **1985**, 83 (2), 735–746.
- (26) Reed, A. E.; Weinhold, F. Natural Bond Orbital Analysis of Near-Hartree–Fock Water Dimer. *J. Chem. Phys.* **1983**, 78 (6), 4066–4073.
- (27) Besler, B. H.; Merz, K. M.; Kollman, P. A. Atomic Charges Derived from Semiempirical Methods. *J. Comput. Chem.* **1990**, 11 (4), 431–439.
- (28) Singh, U. C.; Kollman, P. A. An Approach to Computing Electrostatic Charges for Molecules. *J. Comput. Chem.* **1984**, 5 (2), 129–145.
- (29) Breneman, C. M.; Wiberg, K. B. Determining Atom-Centered Monopoles from Molecular Electrostatic Potentials – The Need for High Sampling Density in Formamide Conformational-Analysis. *J. Comput. Chem.* **1990**, 11 (3), 361–373.
- (30) Dewar, M. J. S.; Maitlis, P. M. Electrophilic Substitution. Part XI. Nitration of Some Six-Membered Nitrogen-Heterocyclic Compounds in Sulfuric Acid. *J. Chem. Soc.* **1957**, 2521–2528.
- (31) Flurichick, K.; Bartolotti, L. Visualizing Properties of Atomic and Molecular-Systems. *J. Mol. Graphics* **1995**, 13 (1), 10–13.
- (32) Bartolotti, L. J.; Ayers, P. W. An Example where Orbital Relaxation Is an Important Contribution to the Fukui Function. *J. Phys. Chem. A* **2005**, 109 (6), 1146–1151.
- (33) We have confirmed that the qualitative features of these plots do not alter when the isodensity surface is moved closer to the molecule. To the eye, plots generated using the 0.001 and 0.002 isodensity surfaces look the same as the ones in Figure 1.
- (34) Berkowitz, M. Density Functional-Approach to Frontier Controlled Reactions. *J. Am. Chem. Soc.* **1987**, 109 (16), 4823–4825.
- (35) Chattaraj, P. K. Chemical Reactivity and Selectivity: Local HSAB Principle versus Frontier Orbital Theory. *J. Phys. Chem. A* **2001**, 105 (2), 511–513.
- (36) Hocquet, A.; Toro-Labbe, A.; Chermette, H. Intramolecular Interactions along the Reaction Path of Keto–Enol Tautomerism: Fukui Functions as Local Softnesses and Charges as Local Hardnesses. *THEOCHEM* **2004**, 686 (1–3), 213–218.
- (37) Because of the slow asymptotic decay of the electrostatic potential and the Fukui potential, plots such as that in Figure 1 do not provide useful information.
- (38) Miller, B. *Advanced Organic Chemistry: Reactions and Mechanisms*; Prentice Hall: Upper Saddle River, NJ, 1998.
- (39) The reader might notice that, with regard to atomic charges, the nitrogen atom and carbon 4 have similar negative charges in the electrostatic charge-fitting schemes (Figure 2a). Note, however, that, once one considers the hydrogen-summed charges (Figure 2b), protonation on the nitrogen is clearly preferred. The protonation of carbon 4 would be associated with the electrophilic aromatic substitution of hydrogen for hydrogen. So even if carbon 4 were protonated, the concentration of the tetrahedral reactive intermediate would be very, very low. It follows that the case where the molecule is protonated at carbon 4 is unlikely to contribute to the overall chemical reactivity in any significant way. The protonation of carbon 4 could be studied by deuterium exchange experiments, but we are unaware of experimental studies of this type.
- (40) Dewar, M. J. S. Heteroaromatic Boron Compounds. *Prog. Boron Chem.* **1964**, 1, 235–263.
- (41) Dewar, M. J. S.; Kubba, V. P. New Heteroaromatic Compounds. VII. Chloro and Bromo Derivatives of 10-Hydroxy-10,9-borazarophenanthrene. *J. Org. Chem.* **1960**, 25, 1722–1724.
- (42) Dewar, M. J. S.; Kubra, V. P. New Heteroaromatic Compounds IV. The Nitration and Chlorination of 10-Methyl-10,9-borazarophenanthrene. *Tetrahedron* **1959**, 7, 213–222.
- (43) Dewar, M. J. S.; Warford, E. W. T. Electrophilic Substitution. III. The Nitration of Phenanthrene. *J. Chem. Soc.* **1956**, 3570–3572.
- (44) Dewar, M. J. S.; Kubba, V. P. New Heteroaromatic Compounds. XI. Friedel–Crafts Acetylation of 10-Methyl- and 10-Hydroxyl-10,9-borazarophenanthrene. *J. Am. Chem. Soc.* **1961**, 83, 1757–1760.
- (45) To the extent that electrophilic attack on the nitrogen atom does occur, it will be associated with molecular decomposition (just like protonation on this site). Though Dewar’s experiments often produced the featured products in high yield, some of the impurities might be due to the decomposition of the starting reagent induced by electrophilic attack on the nitrogen atom. It is impossible to quantify the importance of this process, so we will focus on the reaction pathways for which there is incontrovertible experimental evidence.
- (46) One might argue that, because our model is based on changes in the interaction potential, charges from electrostatic potential fitting are the more natural choice. While we share this view, it is also true that, if one is far enough from the molecule, the charges based on natural population analysis (or any other density-matrix population analysis method) reproduce the electrostatic potential.
- (47) This is especially true in Tables 2 and 3 but not as true for Table 1.
- (48) We attempted to add a sodium cation near the nitrogen atom to mimic the complexation. If there is a potential energy well in this area, it seems to be very shallow: in our calculations, the cation always either dissociated or migrated to the top of one of the aromatic rings.
- (49) Again, naive application of the reactivity indicator sometimes indicates that ipso attack is favored. The carbon of the methyl group is also predicted to be rather reactive, but electrophilic substitution at this carbon cannot occur because of the absence of the electrofuge. In the text and in the tables, we focus our treatment on the ring carbons that are subject to substitution, carbons 1–8.

CT6001658